

**New signals of an  $R$ -parity violating model of neutrino mass at the Fermilab Tevatron**

Amitava Datta\* and Sujoy Poddar†

*Department of Physics, Jadavpur University, Kolkata- 700 032, India*

(Received 20 November 2006; published 19 April 2007)

In a variety of models of neutrino masses and mixings the lighter top squark decays into competing  $R$ -parity violating and  $R$ -parity conserving channels. Using PYTHIA we have estimated in a model independent way the minimum value of  $P \equiv \text{BR}(\tilde{t}_1 \rightarrow c\tilde{\chi}_1^0) \times \text{BR}(\tilde{t}_1 \rightarrow l_i^+ b)$ , where  $l_i = e^+$  and  $\mu^+$ , corresponding to an observable signal involving the final state  $ll + \text{jets} + \cancel{E}_T$  (carried by the neutrinos from the  $\tilde{\chi}_1^0$  decay) at Tevatron Run II. For the kinematical cuts designed in this paper  $P$  depends on  $m_{\tilde{t}_1}$  only. We then compute  $P$  for representative choices of the model parameters constrained by the oscillation data and find that over a significant region of the allowed parameter space  $P$  is indeed larger than  $P_{\min}$ . This signal is complementary to the dilepton + dijet signal studied in several earlier experimental and phenomenological analyses and may be observed even if  $\text{BR}(\tilde{t}_1 \rightarrow l_i^+ b)$  is an order of magnitude smaller than  $\text{BR}(\tilde{t}_1 \rightarrow c\tilde{\chi}_1^0)$ . The invariant mass distribution of the hardest lepton and the hardest jet may determine  $m_{\tilde{t}_1}$  and reveal the lepton number violating nature of the underlying interaction. The invariant mass distribution of the two lowest energy jets may determine  $m_{\tilde{\chi}_1^0}$ .

DOI: [10.1103/PhysRevD.75.075013](https://doi.org/10.1103/PhysRevD.75.075013)

PACS numbers: 11.30.Pb, 13.85.-t, 14.60.Pq, 14.80.Ly

**I. INTRODUCTION**

Neutrino oscillations in different experiments have [1] established that the neutrinos have tiny masses, several orders of magnitude smaller than any other fermion mass in the standard model (SM) with massless neutrinos. Massive Dirac neutrinos can be accommodated in the SM if right-handed neutrinos are introduced as SU(2) singlets. But the corresponding Yukawa couplings must be unnaturally small. There are several more aesthetic mechanisms of introducing neutrino masses. We shall briefly review below two popular approaches based on supersymmetry (SUSY) [2] and their possible impacts on the high priority program of SUSY search at high energy accelerators—on the current and future experiments at Tevatron Run II, in particular.

The seesaw mechanism [3] in a grand unified theory (GUT) [4], with or without SUSY [2], offers a natural explanation of small neutrino masses provided the neutrinos are Majorana fermions. One need not fine-tune the Dirac masses to unnaturally small magnitudes. Instead a typical neutrino Dirac (Majorana) mass in this model is assumed to be of the order of the electroweak scale (GUT scale ( $M_G$ )). The physical neutrino masses turn out to be proportional to the ratio of these scales of widely different magnitudes and are, therefore, naturally suppressed.

The observation of neutrinoless double beta decay [5] will provide a strong indirect evidence in favor of the Majorana neutrinos. Another hallmark of any GUT is the proton decay [4] which has not been observed so far. However, all nonsupersymmetric GUTs suffer from the naturalness problem [2] which destabilizes the mass of

the Higgs boson essentially due to the same large hierarchy of the two mass scales responsible for the seesaw.

A supersymmetric GUT (SUSYGUT) cures the hierarchy problem provided the masses of the sparticles (the supersymmetric partners of the SM particles) are  $\mathcal{O}$  (1 TeV). Thus the exciting program of sparticle searches and the reconstruction of their masses at the ongoing (Tevatron Run II) and the upcoming (the Large Hadron Collider (LHC) or the International Linear Collider (ILC)) accelerator experiments have the potential of testing SUSY. Furthermore, in simple grand desert type models SUSY indeed facilitates the unification of the three couplings of the SM at a scale compatible with the current constraints from proton decay.

It should, however, be emphasized that in the most general framework with a chosen GUT group the neutrino masses and mixing angles involve many unknown free parameters (e.g., the elements of the Dirac and Majorana mass matrices). Collider experiments provide very little information on this sector. On the other hand Neutrino data alone cannot fully determine these parameters unless additional assumptions are introduced to simplify the neutrino mass matrix [6]. Such assumptions involve the minimal choice of Higgs multiplet in a GUT, imposition of additional discrete symmetries, etc. Thus the observation of both neutrinoless double beta decay and proton decay along with the discovery of sparticles with masses at the TeV scale may at best be regarded as a circumstantial evidence of an underlying SUSYGUT. There is no simple way of relating the measured sparticle masses with the physics of the neutrino sector.

Although theoretically the idea of unification of the couplings is rather appealing there is no compelling experimental evidence in favor of it. More importantly if neutrinoless double beta decay is observed but the proton

\*Electronic address: [adatta@juphys.ernet.in](mailto:adatta@juphys.ernet.in)†Electronic address: [sujoy@juphys.ernet.in](mailto:sujoy@juphys.ernet.in)

decay remains illusive, the case for an alternative theory would be strengthened. Such a theory is provided by the  $R$ -parity violating (RPV) supersymmetry, where  $R$ -parity is a discrete symmetry under which the particles and the sparticles transform differently [7]. It should be noted that the minimal supersymmetric extension of the SM (MSSM) naturally contains an  $R$ -parity conserving (RPC) as well as an RPV sector [2]. But the couplings in the latter sector violate both lepton number and baryon number resulting in catastrophic proton decays. Thus one option is to impose  $R$ -parity as a symmetry and eliminate all RPV couplings. This model is generally referred to as the RPC MSSM.

But there is an alternative. If either baryon number or lepton number conservation but not both is required by imposing appropriate discrete symmetries then the catastrophic proton decay is suppressed. Such models are usually referred to as the RPV MSSM.

The lepton number violating version of the RPV MSSM is more appealing since it naturally leads to Majorana masses of the neutrinos [7–9] and neutrinoless double beta decay [7].<sup>1</sup>

More importantly, the observables in the neutrino sector in this depend not only on the RPV parameters but also on the RPC ones (including the sparticle masses). Thus the precise determination of the neutrino masses and mixing angles in neutrino oscillations and related experiments on the one hand and the measurement of sparticle masses and branching ratios (BRs) at accelerator experiments on the other, can indeed test this model quantitatively. In addition the collider signatures of this model are quite distinct from that of the RPC model (see below). In this paper our focus will be on a novel signature of an RPV model of  $\nu$  mass which can be probed at Run II of the Tevatron collider.

In the RPC MSSM the lightest supersymmetric particle (LSP) is necessarily weakly interacting, stable and, as a consequence, a carrier of missing transverse energy ( $\cancel{E}_T$ ). This  $\cancel{E}_T$  is a hallmark of RPC SUSY. In contrast the LSP is necessarily unstable and decays into RPV channels, violating lepton number in the model under consideration. In addition other sparticles can also decay into lepton number violating modes providing very novel collider signatures. The BRs of the latter decays, however, depend on the relative magnitudes of their widths and that of the competing RPC channels. Thanks to the LSP decay the multiplicity of particles in any event is usually much larger compared to the corresponding event in RPC SUSY containing the stable LSP. Moreover, since the LSP is not a carrier of  $\cancel{E}_T$  the reconstruction of sparticle masses appears to be less problematic in an RPV model. We shall consider a few examples of such reconstructions later.

<sup>1</sup>The RPV MSSM can be accommodated in a GUT by introducing, e.g., nonrenormalizable higher dimensional operators; see the concluding section for further discussions and references.

Apparently the stringent constraints from the neutrino data (discussed below) imply that the RPV couplings must be highly suppressed. This in turn suggests that the BRs of the lepton number violating decays of sparticles other than the LSP will be very small compared to the competing RPC decays. One notable exception, however, is the direct RPV decay of the lighter top squark ( $\tilde{t}_1$ ) [10–13], if it happens to be the next lightest supersymmetric particle (NLSP) while the lightest neutralino ( $\tilde{\chi}_1^0$ ) is the LSP. The  $\tilde{t}_1$ -NLSP assumption is theoretically well motivated due to potentially large mixing effects in the top squark mass matrix [2]. In this case the RPC decays of  $\tilde{t}_1$  occur only in higher orders of perturbation theory and are also suppressed (to be elaborated later). Thus they can naturally compete with the RPV decays even if the latter modes have highly suppressed widths as indicated by the neutrino data. Thus the competition among different decay modes of the lighter top squark, which may be the only strongly interacting sparticle within the striking range of Tevatron Run II, is a hallmark of RPV models of neutrino mass [13].

No signal of either RPC or RPV has been observed so far. Thus constraints on the RPV parameters [7,14] have been obtained from the experimental data. As in the case of a SUSYGUT, the most general RPV framework has too many parameters. Thus one usually considers some benchmark scenarios, each consisting of a minimal set of RPV parameters at the weak scale [15,16], which can produce an acceptable neutrino mass matrix consistent with the oscillation data.

Among the examples in Ref. [15], we have focused on a specific model with three trilinear couplings  $\lambda'_{i33}$  (where  $i = 1, 2, 3$  is the lepton generation index) which can trigger  $\tilde{t}_1$  decays and three bilinear RPV parameters  $\mu_i$  at the weak scale. With the above couplings the neutrino masses turn out to be proportional to  $m_b^2$ . A brief review of this model along with notations used here may be found in Sec. 2 of [17].

The stringent upper bounds [15,17] on the trilinear (bilinear) couplings from neutrino data are  $\sim 10^{-4}$  ( $\sim 10^{-4}$  GeV). Thus almost all collider signatures arising from these couplings except the LSP decay are expected to be unobservable. As already mentioned, a notable exception could be the direct RPV decay of the  $\tilde{t}_1$ -NLSP via a  $\lambda'_{i33}$  type coupling [12,13] into a  $b$ -quark and a charged lepton,

$$\tilde{t}_1 \rightarrow l_i^+ b, \quad (1)$$

where  $i = e, \mu, \text{ or } \tau$ .

This is so because the competing RPC decay modes in this case are (i) the loop induced decay [18]

$$\tilde{t}_1 \rightarrow c \tilde{\chi}_1^0 \quad (2)$$

and (ii) the four-body decay [19]

$$\tilde{t}_1 \rightarrow b \tilde{\chi}_1^0 f \bar{f}', \quad (3)$$

where  $f\text{-}\bar{f}'$  refers to a pair of light fermions. The last two decays occur only in higher orders of perturbation theory and, consequently, their widths are also highly suppressed. It may be recalled that for relatively large values of  $\tan\beta$  the loop induced decay overwhelms both the RPV decay [13] and the four-body decay [19–21].

In the earlier experimental and phenomenological analyses signals from the pair production of  $\tilde{\tau}_1\text{-}\tilde{\tau}_1^*$  [11–13] followed by RPV decays of both were considered. The model independent minimum observable branching ratio (MOBR) of the channel  $\tilde{\tau}_1 \rightarrow e^+ b$  for Tevatron Run II was also estimated as a function of the lighter top squark mass ( $m_{\tilde{\tau}_1}$ ) [13] by considering the dilepton + dijet signal. We shall review these limits and their consequences in a later section. Moreover, it was also demonstrated that by reconstructing the two lepton-jet invariant masses the lepton number violating nature of the decay can be directly established [13] for a variety of  $m_{\tilde{\tau}_1}$ .

In this work we shall concentrate on a new signal which arises if one member of the  $\tilde{\tau}_1\text{-}\tilde{\tau}_1^*$  pair decays via the RPV channel into an electron or a muon while the other decays via the loop induced channel (Eq. (2)). The second decay is assumed to be followed by the LSP decay via the modes

$$\tilde{\chi}_1^0 \rightarrow \nu_i b \bar{b}; \quad i = 1, 2, 3. \quad (4)$$

The modes in Eq. (4) indeed occur with a combined BR of 100% in all models provided the LSP mass  $m_{\tilde{\chi}_1^0}$  is smaller than  $m_W$  (the  $W$  boson mass) so that its decays into  $W$ ,  $Z$ , or  $t$  are kinematically forbidden. In addition it holds to a high degree of accuracy for any  $m_{\tilde{\chi}_1^0}$  if the Higgsino components of the LSP are highly suppressed (e.g., if it is almost a pure bino) and it is lighter than  $m_t$ .<sup>2</sup> Thus the signal consists of a very energetic lepton accompanied by several jets (we do not employ flavor tagging) plus a moderate amount of missing energy carried by the neutrinos. We have generated the signal events by using PYTHIA (version 6206) [22]. The background events, discussed in detail in the next section, are generated either directly by PYTHIA or by interfacing PYTHIA and CalcHEP (version 2.3.7) [23]. We then introduce kinematical cuts which optimally suppress the backgrounds. Finally we define the model independent product branching ratio (PBR)

$$P \equiv \text{BR}(\tilde{\tau}_1 \rightarrow l^+ b) \times \text{BR}(\tilde{\tau}_1^* \rightarrow \bar{c} \tilde{\chi}_1^0), \quad (5)$$

where  $\text{BR}(\tilde{\tau}_1 \rightarrow l^+ b) \equiv \text{BR}(\tilde{\tau}_1 \rightarrow e^+ b) + \text{BR}(\tilde{\tau}_1 \rightarrow \mu^+ b)$  and  $\tilde{\chi}_1^0$  is assumed to decay into a pair of jets and missing energy (Eq. (4)) with 100% BR. Our simulations estimate the minimum value of  $P(P_{\min})$  as a function of  $m_{\tilde{\tau}_1}$  corresponding to an observable signal. These estimates are for an integrated luminosity of  $9 \text{ fb}^{-1}$  and  $S/\sqrt{B} = 5$  where  $S$  and  $B$  are the total number of signal and background

events. We have used the top squark pair production cross section as given by QCD [24] as an input.

We have also examined the invariant mass of the most energetic lepton and jet in the signal for various  $m_{\tilde{\tau}_1}$ . The resulting distribution peaks around the input value of  $m_{\tilde{\tau}_1}$ . This illustrates that the combinatorial backgrounds are not very damaging. The peak, if observed, will unambiguously demonstrate the lepton number violating nature of the underlying interaction.

Our estimates also establish that the signals proposed in [13] and that proposed in this paper are complementary. While the former happens to be the most promising search channel if the RPV BR dominates over that of the loop induced decay, the latter can potentially reveal the presence of RPV interactions even if the loop decay overwhelms the RPV decays. These points will be further illustrated in the subsequent sections with numerical examples.

We then turn our attention to some specific models. We compute  $P$  in these models for the entire RPV parameter space allowed by the oscillation data and compare the results with  $P_{\min}$  estimated by our Monte Carlo. We find that for top squark masses within the striking range of the Tevatron, a large region of the allowed parameter space (APS) yields  $P$  greater than the estimated  $P_{\min}$ . We have also checked that in significant regions of this parameter space the  $\text{BR}(\tilde{\tau}_1 \rightarrow l_i^+ b)$  is in fact smaller than the estimated MOBR in [13] or the updated value given in Sec. III. Thus the signal introduced in this paper is indeed complementary to the ones studied earlier and may turn out to be the main discovery channel of  $\tilde{\tau}_1$ .

The plan of the paper is as follows. In Sec. II we present our Monte Carlo studies of the signal and the backgrounds. This is followed by the main results of this paper: the model independent estimates of  $P_{\min}$  as a function of  $m_{\tilde{\tau}_1}$ . A comparison of the viability of this signal *vis-à-vis* that of [13] is also included. In Sec. III we compute the parameter  $P$  in some specific models and revise the estimated MOBR in [13] for representative parameter spaces consistent with neutrino oscillation data. This study establishes that the two signals are indeed complementary. Our conclusions and future outlooks are summarized in the last section.

## II. THE SIGNAL AND THE SM BACKGROUND

We have simulated the signal described in the introduction by generating  $10^5$  events using PYTHIA. The most energetic  $l\text{-}b$  pair in the final state comes most of the time from the direct decay of  $\tilde{\tau}_1$ . The kinematics of this pair is, therefore, independent of  $m_{\tilde{\chi}_1^0}$ . Using this feature we have shown that it is possible to choose the optimal kinematical cuts in such a way that the efficiency of these cuts is practically independent of  $m_{\tilde{\chi}_1^0}$ . The size of our signal is completely determined by (i) the cross section of  $\tilde{\tau}_1$  pair production as given by QCD [24] and the efficiency which

<sup>2</sup>See Sec. III for further details.

TABLE I. Leading order cross sections of the simulated backgrounds and the efficiencies of the cuts  $C_1$ ,  $C_2$ , and  $C_3$ .

Backgrounds	$\sigma$ (pb)	$\epsilon_1$	$N_1$	$\epsilon_2$	$N_2$	$\epsilon_3$	$N_3$
$t\bar{t}$	3.73	0.0179	601.0	0.7791	468.3	0.9327	436.8
$W^+W^-$	9.51	0.00623	533.2	0.2055	109.5	0.7188	78.7
$WZ$	1.16	0.00541	56.5	0.2683	14.9	0.6831	10.4
$WH$	0.11	0.0093	9.2	0.3211	3.0	0.6286	1.9
$b\bar{b}$	$2.82 \times 10^7$	0.0	0.0	0.0	0.0	0.0	0.0
$t\bar{b} + \bar{t}b$	0.33	0.00824	24.47	0.3398	8.31	0.8	6.65
$Wb\bar{b}$	11.6	.00126	131.5	0.119	15.7	0.6667	10.5
$Wu\bar{u}$	73.5	0.00103	681.3	0.2136	145.5	0.9545	138.9

depends only on  $m_{\tilde{t}_1}$  among the SUSY parameters and (ii) the model independent input value of  $P$  (Eq. (5)). We have considered the following backgrounds:

- (1)  $t\bar{t}$ ,
- (2)  $W^+W^-$ ,
- (3)  $WZ$ ,
- (4)  $WH$ ,
- (5)  $b\bar{b}$ ,
- (6)  $t\bar{b} + \bar{t}b$ ,
- (7)  $W + 2j$ .

Backgrounds 1 to 5 have been simulated by PYTHIA. Backgrounds 6 and 7 have been generated by CalcHEP at the parton level. Subsequently initial and final state radiation, hadronization, decay, and jet formation have been implemented by interfacing with PYTHIA. All cross sections are calculated by CalcHEP in the leading order using the CTEQ6M parton density functions [25] using the four flavor scheme. The next-to-leading order (NLO) corrections would modify both the signal and the backgrounds by the appropriate  $K$ -factors. For example, the recent QCD prediction for the  $K$ -factor for the  $t\bar{t}$  cross section, the most dominant background (see Table I), is 0.94 to 1.52 depending on the choice of the renormalization scale in the leading order cross section [26]. The corresponding number for the signal is  $\approx 1.3$  [27]. Since our main result (the estimated  $P_{\min}$ ) is based on the ratio  $S/\sqrt{B}$ , we believe that neglecting the NLO corrections would not change our conclusions drastically.

For the background from  $Wb\bar{b}$ ,  $\sigma$  has been computed with nominal cuts of  $P_T > 3$  GeV and  $|\eta| < 4.0$  on the parton jets. This is to eliminate the soft and collinear processes which are important for the NLO calculation. Here our main aim is to generate events with high  $p_T$ , central jets which can contribute to the background surviving the cuts listed below. We have checked that reasonable variations of these nominal cuts do not influence the final results.

The backgrounds from  $Ws\bar{s}$  and  $Wc\bar{c}$  have not been simulated separately since flavor tagging is not included in our selection criteria and for our cuts these contributions are expected to be similar to that of  $Wb\bar{b}$ . Similarly the  $Wd\bar{d}$  and  $Wu\bar{u}$  backgrounds computed with the same

nominal cuts as above are practically identical and only one of them has been simulated. Unless otherwise mentioned contributions of  $W$ 's of both signs are included in Table I.

We present the kinematical cuts and their efficiencies for the signal and the backgrounds in Tables I and II for  $m_{\tilde{t}_1} = 180$  GeV. The cuts ( $C_1$ - $C_3$ ) are as follows:

- (1)  $C_1$ : Only events having an isolated lepton ( $e$  or  $\mu$  of either charge) with  $\Delta R(l, j) > 0.5$ ,  $|\eta_l| < 2.5$ , and  $P_T > 105$  GeV are accepted. Here  $\Delta R(m, n) = \sqrt{\Delta\phi^2 + \Delta\eta^2}$ ,  $m, n$  stand for either a lepton ( $l$ ) or a jet ( $j$ ).
- (2)  $C_2$ : The number of jets in an accepted event is required to be  $n_j > 2$ , where, jets are selected by the toy calorimeter of PYTHIA if  $E_T^j > 12$  GeV,  $|\eta_j| < 2.4$ , and  $\Delta R(j_1, j_2) > 0.5$ .
- (3)  $C_3$ : Events with the invariant mass of the two highest  $P_T$  jets lying between  $100 \text{ GeV} < M_{j_1 j_2} < 70 \text{ GeV}$  are rejected.

The cuts are applied in the order shown in the table. The efficiencies ( $\epsilon_i$ 's) in Tables I and II are defined as  $N_i^s = \epsilon_i N_{i-1}^s$ , where  $i = 1, 2, 3$ ,  $N_i^s$  is the number of events selected after the  $i$ th cut out of  $N_0^s$  generated events. The expected number of events  $N_i$  in Table I, where  $i = 1, 2, 3$ , is obtained by multiplying the combined efficiency  $\epsilon (= \epsilon_1 \epsilon_2 \dots \epsilon_i)$  with  $\sigma \mathcal{L}$ .

The expected number of signal events  $S$  (considering final states with both  $e^\pm$  and  $\mu^\pm$ ) is given by  $4 \cdot \epsilon P \sigma \mathcal{L}$ , where  $P$  is the product BR (see Eq. (5)) sufficient to yield  $S/\sqrt{B} = 5$ . In our simulations  $\epsilon$  has been computed by generating ( $\tilde{t}_1 \rightarrow e^+ b$ ) events only and we have assumed that the efficiency is the same for electrons and muons. Out of the three  $P$ 's estimated in Table II the minimum ( $P_{\min}$ ) is

TABLE II. The signal cross section for  $m_{\tilde{t}_1} = 180$  GeV and efficiencies of the cuts  $C_1$ ,  $C_2$ , and  $C_3$ . We have computed  $P$  (see Eq. (5)) after each cut from Eq. (6) by requiring  $S/\sqrt{B} = 5$ .

Signal	$\sigma$ (pb)	$\epsilon_1$	$P$	$\epsilon_2$	$P$	$\epsilon_3$	$P$
$\tilde{t}_1 \tilde{t}_1^*$	0.41	0.30473	0.060	0.9116	0.037	0.7702	0.047

obtained by the combination of  $C_1$  and  $C_2$  only. This conclusion holds for other choices of  $m_{\tilde{t}_1}$  (within the kinematic reach of Tevatron Run II) as well. We have tried a variety of additional selection criteria including  $b$ -tagging not shown in Table I. For example, we have tried various lower  $P_T$  cuts on the hardest jet. But the corresponding  $P_{\min}$  turns out to be weaker. On the other hand a lower  $P_T$  cut on second hardest jet yields a  $P$  sensitive to the LSP mass and introduces model dependence. We therefore conclude that the combination of  $C_1$  and  $C_2$  is the optimal one.

In Table II  $P$  (Eq. (5)) is calculated by the formula:

$$P = \frac{5\sqrt{\mathcal{L}\Sigma\sigma^b\epsilon^b}}{4\mathcal{L}\sigma(\tilde{t}_1\tilde{t}_1^*)\epsilon}, \quad (6)$$

where  $\sigma^b$  and  $\epsilon^b$  denote the cross section and the combined efficiency (i.e.,  $\epsilon_b \equiv N_{\text{selected}}/N_{\text{generated}} = \epsilon_1\epsilon_2$ ) of the background of type  $b$ . Similarly  $\epsilon$  is the combined efficiency for the signal. The integrated luminosity  $\mathcal{L}$  is taken to be  $9 \text{ fb}^{-1}$ .

We have also computed the backgrounds due to one valence quark and one sea quark. Some typical process and the corresponding number of background events (given in parentheses) subject to the cuts  $C_1$  and  $C_2$  are:  $W^+dd + W^-\bar{d}\bar{d}$  (12.4) and  $W^+ud + W^-\bar{u}\bar{d}$  (18.7). The corresponding  $\sigma$ s have been calculated by applying nominal cuts of  $P_T > 3 \text{ GeV}$  and  $|\eta| < 4.5$  on the parton jets. It can be readily checked that these additional backgrounds hardly affect the estimated  $P_{\min}$ .

We present in Fig. 1  $P_{\min}$  as a function of  $m_{\tilde{t}_1}$  for  $m_{\tilde{\chi}_1^0} = 120 \text{ GeV}$ . In Fig. 2 the variation of  $P_{\min}$  with  $m_{\tilde{\chi}_1^0}$  is shown for  $m_{\tilde{t}_1} = 180 \text{ GeV}$ . It follows that  $P_{\min}$  is almost insensitive to the LSP mass as claimed above.

We present in Fig. 3 the distribution (unnormalized) of invariant mass of the highest  $P_T$  lepton and the highest  $P_T$  jet in the signal for  $m_{\tilde{t}_1} = 180 \text{ GeV}$  and  $m_{\tilde{\chi}_1^0} = 120 \text{ GeV}$ .

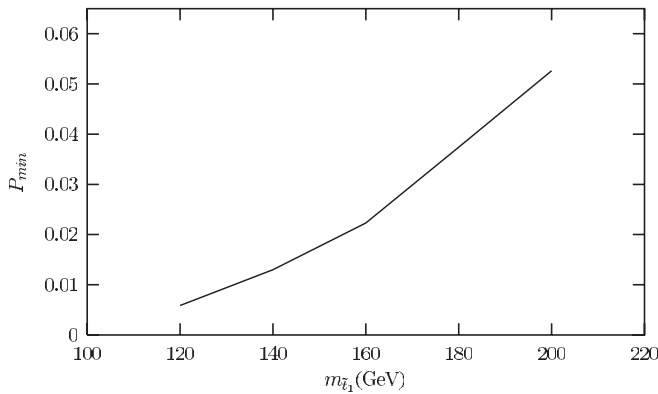


FIG. 1. The model independent minimum value of the parameter  $P \equiv \text{BR}(\tilde{t}_1 \rightarrow c\tilde{\chi}_1^0) \times \text{BR}(\tilde{t}_1 \rightarrow l^+b)$ , where  $l^+ = e^+$  and  $\mu^+$ , observable at Tevatron Run II via  $1l + \text{jets} + \cancel{E}_T$  channel as a function of  $m_{\tilde{t}_1}$ .

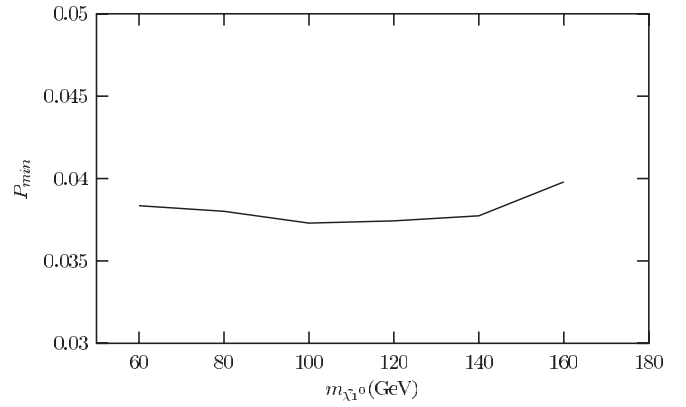


FIG. 2. The variation of  $P_{\min}$  (see the caption of Fig. 1) with  $m_{\tilde{\chi}_1^0}$ .

In spite of the presence of multiple jets in the signal, the combinatorial background does not obscure the peak at the input value of  $m_{\tilde{t}_1}$ . In principle  $m_{\tilde{t}_1}$  can be determined from this distribution and the lepton number violating nature of the underlying interaction can be established. Whether this peak will stand over the background depends on the actual value of  $P$  and  $m_{\tilde{t}_1}$ . The issue of the observability of this peak at Tevatron, therefore, cannot be settled at the moment.

In Fig. 4 we plot the distribution (unnormalized) of the invariant mass of the two lowest  $P_T$  jets in the signal, which comes most of the time from LSP decay. The mass of the LSP can be estimated in principle from the upper edge of this distribution. Again the combinatorial backgrounds obscure the edge a little bit but are not particularly severe.

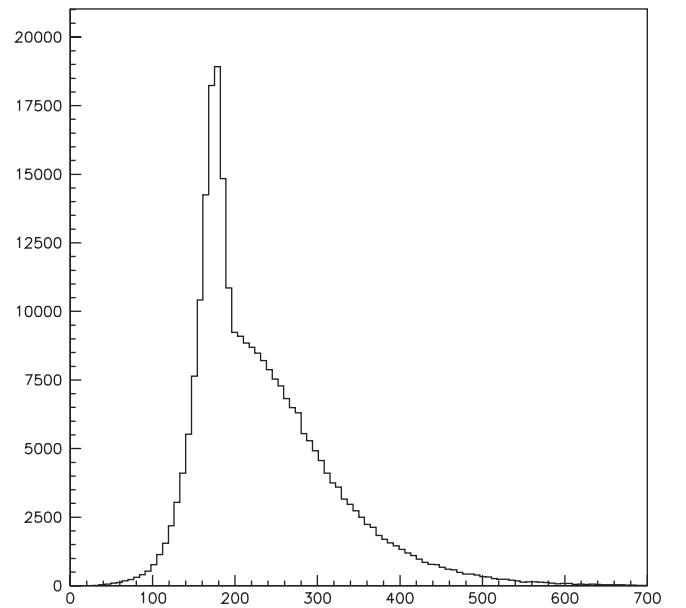


FIG. 3. The invariant mass distribution of the hardest jet and the hardest lepton in the signal for  $m_{\tilde{t}_1} = 180 \text{ GeV}$ .

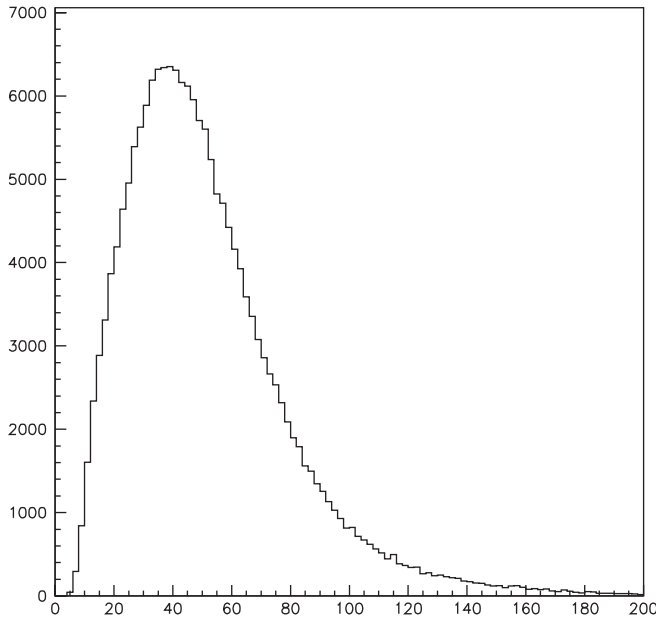


FIG. 4. The invariant mass distribution of the lowest two  $P_T$  jets in the signal for  $m_{\tilde{\chi}_1^0} \approx 120$  GeV.

Throughout this section we assume  $\text{BR}(\tilde{\chi}_1^0 \rightarrow \nu b \bar{b}) = 1.0$ . However, if this assumption is not strictly true, e.g., due to the presence of several rare decay modes of the LSP due to chargino-charge lepton or neutralino-neutrino mixing (see the next section) which we have neglected, then  $P_{\min}$  in Fig. 1 should be interpreted as the minimum value of the product  $P \times \text{BR}(\tilde{\chi}_1^0 \rightarrow \nu b \bar{b})$ .

### III. CALCULATION OF THE PRODUCT BRANCHING RATIO IN THE MODEL OF $m_\nu$

In this section we shall calculate  $P$  in some realistic models of neutrino mass constrained by the neutrino oscillation data and examine whether the predictions exceed  $P_{\min}$  estimated in the last section. Our main aim is to illustrate that the Run II data is sufficiently sensitive to probe these models and not to make an exhaustive study of all possible models.

The collider signatures considered in the last section arise only in models with some nonvanishing trilinear  $\lambda'_{ij}$  type couplings. However, consistency with neutrino oscillation data require the introduction of more RPV parameters (bilinear superpotential terms, bilinear soft breaking terms, etc). In fact the list of possible choices is quite long. It is expected that the constraints on the  $\lambda'$  couplings in the most general model imposed by the  $\nu$ -oscillation data will be considerably weaker. On the other hand for large  $\lambda'$  couplings the dilepton + dijet signal studied in earlier works [13] has a better discovery potential. Thus we have restricted ourselves to models with a minimal set of parameters capable of explaining the oscillation data with rather stringent constraints on the  $\lambda'$  couplings.

The benchmark scenario studied in this paper was proposed in Ref. [15] where it was confronted with the then  $\nu$ -oscillation data. We work in a basis where the sneutrino vacuum expectation values (vevs) are zero. It is assumed that in this basis only three nonzero bilinear ( $\mu_i$ ) and three trilinear ( $\lambda'_{i33}$ ) couplings, all defined at the weak scale, are numerically significant. In this framework the neutrino mass matrix receives contributions both at the tree and one-loop level. It should be emphasized that the tree-level mass matrix yields two massless neutrinos. Thus the interplay of the tree-level and one-loop mass matrices is essential for consistency with the oscillation data.

The chargino-charge lepton, the neutralino-neutrino, and other relevant mixing matrices in this basis may be found in [9]. In principle the diagonalization of these matrices may induce additional lepton number violating couplings which can affect the top squark and LSP decays considered in this paper. However, we shall show at the end of this section that the decays triggered by such induced couplings are highly suppressed either kinematically or dynamically in a wide variety of models. As a result the approximation that the decays of the top squark NLSP are driven by the  $\lambda'_{i33}$  couplings only is justified. The decay of the LSP requires a more careful handling and will be taken up at the end of this section.

In [15] only the upper bounds on  $\lambda'_{i33}$  couplings as obtained from the neutrino oscillation data were reported. It was shown in Refs. [12,13] that the BR limits of the RPV decay of the  $\tilde{t}_1$ -NLSP sensitive to Tevatron Run I data (the MOBR that can be probed by Run II data) correspond to  $\lambda'$ 's which are close to the above upper bounds. In Ref. [17] the six RPV parameters in these models were randomly generated and the neutrino masses and mixing angles were computed for some well-motivated choices of the RPC parameters. Comparing these with more recent oscillation data [28] a remarkably small allowed parameter space was obtained. It was also shown in [17] that there are six generic RPV scenarios consistent with the oscillation data [28]. They are:

- (a)  $\mu_1 \ll \mu_2, \mu_3$ :
  - (a<sub>1</sub>)  $\lambda'_{333} > \lambda'_{133} \geq \lambda'_{233}$
  - (a<sub>2</sub>)  $\lambda'_{233} > \lambda'_{133} \geq \lambda'_{333}$
- (b)  $\mu_2 \ll \mu_1, \mu_3$ :
  - (b<sub>1</sub>)  $\lambda'_{133} \approx \lambda'_{233} \gg \lambda'_{333}$
  - (b<sub>2</sub>)  $\lambda'_{233} > \lambda'_{333} \gg \lambda'_{133}$
- (c)  $\mu_3 \ll \mu_1, \mu_2$ :
  - (c<sub>1</sub>)  $\lambda'_{333} > \lambda'_{133} \gg \lambda'_{233}$
  - (c<sub>2</sub>)  $\lambda'_{333} > \lambda'_{233} \gg \lambda'_{133}$

Each scenario has its characteristic hierarchy among the three leptonic BRs of  $\tilde{t}_1$  (see Eq. (1)). We focus on scenarios (b<sub>1</sub>) and (b<sub>2</sub>) which correspond to relatively large BR for the decay channel in Eq. (1) with  $l_i = e$  or  $\mu$ . However, in addition to the tree-level and  $\lambda'$ - $\lambda'$  loop contributions considered in [15] we have included the contribution of the  $\mu$ - $\lambda'$  loops to the  $\nu$ -mass matrix. An approximate form of

the latter can be found in [9,29] (see, e.g., Eq. 35 of Ref. [9]). The inclusion of the new contribution does not drastically alter the nature of RPV parameter space allowed by the  $\nu$ -oscillation data.

In addition to the RPV parameters the neutrino masses and mixing angles depend on RPC parameters. In this paper we shall use the following popular assumptions to reduce the number of free parameters in the RPC sector: (i) At the weak scale the soft breaking mass squared parameters of the  $L$  and  $R$ -type squarks belonging to the third generation are assumed to be the same (the other squark masses are not relevant for computing neutrino masses and mixing angles in this model). (ii) We shall also use the relation  $M_2 \approx 2M_1$  at the weak scale as is the case in models with a unified gaugino mass at  $M_G$ . Here  $M_1$  and  $M_2$  are, respectively, the soft breaking masses of the  $U(1)$  and  $SU(2)$  gauginos, respectively.

The tree-level neutrino mass matrix and, hence, the predicted neutrino masses depends on the parameters of the gaugino sector (through the parameter  $C$  [15,17]). They are  $M_2$ ,  $M_1$ ,  $\mu$  (the higgsino mass parameter), and  $\tan\beta = v_2/v_1$ , where  $v_1$  and  $v_2$  are the vevs for the down type and the up type neutral Higgs bosons, respectively. We remind the reader that for relatively large  $\tan\beta$ s the loop decay overwhelms the RPV decay. We have, therefore, restricted ourselves to  $\tan\beta = 5-8$ .

It is also convenient to classify various models of the RPC sector according to the relative magnitude of  $M_2$  and  $\mu$ . If  $M_1 < M_2 \ll \mu$ , then the lighter chargino ( $\tilde{\chi}_1^\pm$ ), the LSP ( $\tilde{\chi}_1^0$ ), and the second lightest neutralino ( $\tilde{\chi}_2^0$ ) are dominantly gauginos. Such models are referred to as the gauginolike model. On the other hand in the mixed model ( $M_1 < M_2 \approx \mu$ ),  $\tilde{\chi}_1^\pm$  and  $\tilde{\chi}_2^0$  are admixtures of gauginos and Higgsinos. In both the cases, however,  $\tilde{\chi}_1^0$  is almost a bino. There are models with  $M_1, M_2 \gg \mu$  in which  $\tilde{\chi}_1^\pm$ ,  $\tilde{\chi}_1^0$ , and  $\tilde{\chi}_2^0$  are Higgsinolike and all have approximately the same mass ( $\approx \mu$ ). It is difficult to accommodate the top squark NLSP in such models without fine adjustments of the parameters. Thus the LSP decay seems to be the only viable collider signature.

One can also construct models wino or Higgsino dominated LSPs. However, the  $\tilde{t}_1$ -NLSP scenario cannot be naturally accommodated in these frameworks for reasons similar to the one in the last paragraph.

The one-loop mass matrix, on the other hand, depends on the sbottom sector (through the parameter  $K_2$  [15,17]). This parameter decreases for higher values of the common squark mass for the third generation. From the structure of the mass matrix it then appears that for fixed  $C$ , identical neutrino masses and mixing angles can be obtained for higher values of the trilinear couplings if  $K_2$  is decreased. Thus at first sight it seems that arbitrarily large width of the RPV decays may be accommodated for any given neutrino data. This, however, is not correct because of the complicated dependence of the RPV and loop decay BRs of  $\tilde{t}_1$  on

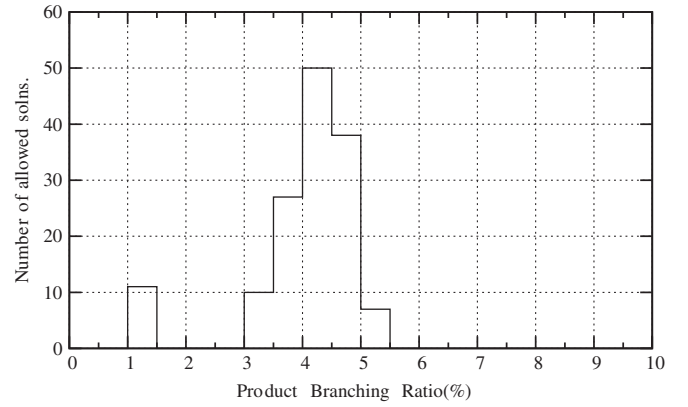


FIG. 5. Number of points in the space allowed by the  $\nu$  oscillation data vs the parameter  $P(\%)$  (Eq. (5)) in the gauginolike model with  $m_{\tilde{t}_1} = 180$  GeV. For the choice of parameters and other details see text.

the RPC parameters and certain theoretical constraints. The common squark mass cannot be increased arbitrarily without violating the top squark NLSP condition. Of course larger values of the trilinear soft breaking term  $A_t$  may restore the NLSP condition. But larger values of  $A_t$  tend to develop a charge color breaking (CCB) minimum of the scalar potential [30]. Finally the pseudoscalar Higgs mass parameter  $M_A$  can be increased to satisfy the CCB condition. But as noted earlier [17] that would enhance the loop decay width as well and suppress the BRs of the RPV decay modes.

We first examine scenario ( $b_2$ ) with the following set of RPC parameters: (A)  $M_1 = 100.0$ ,  $M_2 = 200.0$ ,  $\mu = 320.0$ ,  $\tan\beta = 7.0$ ,  $A_t = 938.0$ ,  $A_b = 300.0$ ,  $M_{\tilde{q}} = 400.0$ ,  $M_{\tilde{l}}$ (common slepton mass) = 350.0, and  $M_A = 600.0$ , where all masses and mass parameters are in GeV.<sup>3</sup> We note in passing that common slepton mass does not enter into the calculation of the BRs and any choice which preserves of  $\tilde{t}_1$ -NLSP condition serves the purpose. For the parameters chosen the loop (four-body) decay BR is  $\approx 50\%$ (34%). Yet the bulk of the APS gives  $P > P_{\min}$ .

In this gauginolike model  $m_{\tilde{t}_1} = 180$  GeV and  $m_{\tilde{\chi}_1^0} = 100$  GeV. The corresponding model independent  $P_{\min}$  is 0.037 (see Fig. 1).

We then randomly generate  $10^7$  sets of the six RPV parameters under consideration and count the sets allowed by the oscillation data. For each point of the APS we compute BRs of the three modes in Eqs. (1)–(3) and get the corresponding  $P$ .

In Fig. 5 we present a histogram of the number of sets allowed by the oscillation data vs  $P$  in the above gauginolike model. It is found that for most of the APS  $P > P_{\min}$ . It

<sup>3</sup>For computing the loop decay BR the mass of the charm squark is required. We assume it to be equal to the third generation common squark mass.

may be recalled that in Ref. [17] it was pointed out that in this model the loop decay BR is much larger than the total RPV decay BR of  $\tilde{\tau}_1$  even for modest values of  $\tan\beta$ . Thus the inclusion of the  $\mu$ - $\lambda'$  loop does not change our conclusion drastically.

In Fig. 6 we present a similar histogram in a mixed model. Here the LSP has a relatively large Higgsino component. Thus the additional decay modes discussed in the introduction (see after Eq. (4)) may open up and reduce the combined BR of the modes in Eq. (4). Hence we have restricted ourselves to  $m_{\tilde{\chi}_1^0} < m_W$ .

We have considered the ( $b_1$ ) scenario for the RPV parameters. The RPC parameters corresponding to this mixed model are chosen to be: (B)  $M_1 = 78.0$ ,  $M_2 = 170.0$ ,  $\mu = 180.0$ ,  $\tan\beta = 8.0$ ,  $A_t = 890.0$ ,  $A_b = 1000.0$ ,  $M_{\tilde{q}} = 375.0$ ,  $M_{\tilde{l}} = 350.0$ ,  $M_A = 300.0$ , where all mass and mass parameters are in GeV. With the above choice of parameters  $m_{\tilde{\tau}_1} = 130$  GeV and  $m_{\tilde{\chi}_1^0}$ . Since, as discussed in Sec. II,  $P_{\min}$  is highly insensitive to  $m_{\tilde{\chi}_1^0}$  one can still use the estimates of Fig. 2. In this case the loop (four-body) decay BR is  $\approx 85\%$  (6.5%). Yet the entire APS gives  $P > P_{\min}$ .

We next compare and contrast the signals considered in this paper and the one discussed in [13]. In the latter work assuming both the  $\tilde{\tau}_1$ s produced at Tevatron Run II decay via the  $\tilde{\tau}_1 \rightarrow e^+ d$  channel the MOBR of this channel was estimated to be 20%. The Drell-Yan process turned out to be the dominant source of background. It was further noted that if  $b$ -tagging is employed the signal will be essentially background free. Using the efficiencies as given in Table [2] of Ref. [13] and including a  $b$ -tagging efficiency of 50% the MOBR for the channel  $\tilde{\tau}_1 \rightarrow e^+ b$  corresponding to ten signal events was estimated to be roughly the same. We define the parameter  $\text{BR}(\tilde{\tau}_1 \rightarrow e^+ b) + \text{BR}(\tilde{\tau}_1 \rightarrow \mu^+ b) \equiv \text{BR}(e + \mu)$ . Following the procedure of Ref. [13] briefly sketched above, we then estimate the minimum

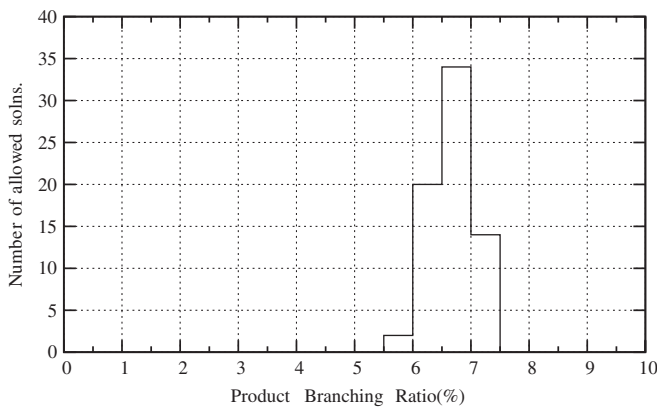


FIG. 6. Number of points in the space allowed by the  $\nu$  oscillation data vs the parameter  $P(\%)$  (Eq. (5)) in the mixed model with  $m_{\tilde{\tau}_1} = 130$  GeV. For the choice of parameters and other details see text.

TABLE III. The minimum observable value of  $\text{BR}(\tilde{\tau}_1 \rightarrow e^+ b) + \text{BR}(\tilde{\tau}_1 \rightarrow \mu^+ b)$  at Tevatron Run II via the dilepton dijet channel for different  $m_{\tilde{\tau}_1}$ .

$m_{\tilde{\tau}_1}$	$\sigma$ (pb)	$\epsilon$	MOBR( $e + \mu$ )
100	13.1	0.0194	0.076
140	2.1	0.0933	0.087
180	0.41	0.2278	0.126
220	0.12	0.3073	0.20

observable value of this parameter ( $\equiv \text{MOBR}(e + \mu)$ ) for  $\mathcal{L} = 9 \text{ fb}^{-1}$ . The results are given in Table III.

We find that in any gauginolike model with  $\tan\beta \geq 6$  the computed  $\text{BR}(e + \mu)$ s turn out to be smaller than the MOBR in Table III practically over the entire APS. For example, in the gauginolike model considered above with  $\tan\beta = 7$ ,  $\text{BR}(e) \approx 0$  and  $\text{BR}(\mu)$  vary from 0.06 to 0.11 (except for a few solutions which correspond to  $\text{BR}(\mu)$  around 0.025). Thus  $\text{BR}(e + \mu)$  is indeed much smaller than the MOBR in Table III for  $m_{\tilde{\tau}_1} = 180$  GeV. However, most of the points in the APS yield  $P$  larger than  $P_{\min}$  (Fig. 5).

For the mixed model considered above the entire APS yields  $P > P_{\min}$ . On the contrary  $\text{BR}(e + \mu)$  is still below the MOBR since the loop and four-body decay BRs are  $\approx 85\%$  and  $\approx 6.5\%$ , respectively. These examples illustrate that the signal in [13] and the one considered in this paper are indeed complimentary.

As noted at the beginning of this section some RPC interactions can induce new lepton number violating interactions of  $\tilde{\tau}_1$  and  $\tilde{\chi}_1^0$  due to chargino-lepton or neutralino-neutrino mixing. These induced interactions can in principle affect the decays of the  $\tilde{\tau}_1$ -NLSP or the LSP considered in Sec. II. For example the RPC vertex  $\tilde{\tau}_1$ - $b$ - $\tilde{W}^\pm$  (or  $\tilde{H}^\pm$ ) may lead to additional lepton number violating couplings of the  $\tilde{\tau}_1$  due to chargino-lepton mixings. Similar induced couplings may arise from  $\tilde{\tau}_1$ - $t$ - $\tilde{W}_3$  (or  $\tilde{B}$  or  $\tilde{H}^0$ ) coupling due to mixing in the neutralino-neutrino sector (these couplings may be relevant only if the  $\tilde{\tau}_1$  is significantly heavier than the  $t$ ). The mixing factors which would suppress the induced couplings can be estimated from the  $5 \times 5$  ( $7 \times 7$ ) chargino-lepton (neutralino-neutrino) mass matrix. The estimated value is  $\mathcal{O}(\mu_i/100 \text{ GeV})$  where 100 GeV is the typical magnitude of an element of the  $2 \times 2$  chargino block or the  $4 \times 4$  neutralino block of the above matrices. Since the largest  $\mu_i$  allowed by the oscillation data is  $\mathcal{O}(10^{-4})$  GeV the mixing factors are estimated to be  $\mathcal{O}(10^{-6})$  or smaller. Moreover, the induced couplings will be additionally suppressed by gauge or Yukawa couplings. On the other hand the smallest  $\lambda'_{133}$  coupling contributing to  $\tilde{\tau}_1$  decay consistent with oscillation data is  $\mathcal{O}(10^{-5})$ . Thus the  $\tilde{\tau}_1$ -NLSP BRs computed by considering  $\lambda'_{133}$  driven decays only are quite reliable. The rough estimates presented here would be substantiated below by results



obtained by numerically diagonalizing the chargino-lepton and neutralino-neutrino mass matrices.

The LSP decays require more careful analysis. The main decay mode considered in this paper (Eq. (4)) is a three-body decay. On the other hand lepton number violating two-body decays of the LSP (the decays  $\tilde{\chi}_1^0 \rightarrow \nu Z$  and  $\tilde{\chi}_1^0 \rightarrow l^+ W$  are examples) can be induced by the  $\tilde{\chi}_1^0$ - $\tilde{W}^+$ - $W^-$  or  $\tilde{\chi}_1^0$ - $\tilde{W}_3$ - $Z$  vertices. However, when the LSP is almost a pure bino, which is the case in the gaugino model, the original RPC couplings are highly suppressed. In addition suppression by the mixing factors discussed in the last paragraph will come into play. Consequently the BRs of the lepton number violating two-body decays of the LSP are  $\mathcal{O}(10.0\%)$  (see below for numerical results). Thus the decay in Eq. (4) indeed occurs with almost 100% BR in this model.

In more general models with the LSP having significant Higgsino components (e.g., in the mixed model) our assumption regarding the LSP decay is valid if  $m_{\tilde{\chi}_1^0} < m_W$ . For heavier LSPs the parameter  $P_{\min}$  in Sec. II should be interpreted as the minimum value of the product  $P \times \text{BR}(\tilde{\chi}_1^0 \rightarrow \nu_i b \bar{b})$  observable at Run II.

We now present some numerical results. We numerically diagonalize the mass matrices in the chargino-lepton or neutralino-neutrino sector for all combinations of RPV parameters allowed by the oscillation data. For the parameter set (A) (the gauginolike model) we find that the maximum amplitude for finding a charge lepton mass eigenstate in a  $\tilde{W}^\pm$  or  $\tilde{H}^\pm$  is  $3.3 \times 10^{-6}$ . The corresponding  $\lambda'_{233}$ , responsible for the  $\tilde{\tau}_1$  or LSP decay signal, is  $8.6 \times 10^{-5}$ . Similarly the maximum amplitude for finding a neutrino mass eigenstate in a  $\tilde{B}$ ,  $\tilde{W}_3$ , or  $\tilde{H}^0$  is  $3.6 \times 10^{-6}$ . The corresponding  $\lambda'_{233}$  is  $8.6 \times 10^{-5}$ . Using the induced couplings in this scenario as given above, the mixings in the RPC chargino and neutralino mass matrices and the widths of the modes ( $\tilde{\chi}_i^0 \rightarrow Z \tilde{\chi}_j^0$ ) and ( $\tilde{\chi}_i^0 \rightarrow W^\pm l_j^\mp$ ) given, e.g., in [31] Eq. 15 to Eq. 21, we find that  $\text{BR}(\tilde{\chi}_i^0 \rightarrow Z \nu_j) = 13.0\%$  and  $\text{BR}(\tilde{\chi}_i^0 \rightarrow W^\pm l_j) = 1.0\%$ .

#### IV. CONCLUSION

In conclusion we reiterate that the  $ll + \text{jets}(\geq 3) + \cancel{E}_T$  signal arising from RPC and RPV decays of  $\tilde{\tau}_1$ - $\tilde{\tau}_1^*$  pairs produced at the Tevatron is a promising channel for probing a class of RPV models of neutrino mass. For a set of kinematical cuts suitably optimized in this paper the size of this signal is essentially controlled by the production cross section of the  $\tilde{\tau}_1$ - $\tilde{\tau}_1^*$  pair as given by QCD and the parameter  $P$  (see Eq. (5)). Using Monte Carlo simulations we have obtained model independent estimates of  $P_{\min}$  for different  $m_{\tilde{\tau}_1}$ s corresponding to an observable signal for an integrated luminosity of  $9 \text{ fb}^{-1}$  (see Fig. 1). The efficiencies of the cuts are entirely controlled by the kinematics of the lepton and the jet with highest  $E_T$  which most of the time come directly from the RPV decay of the  $\tilde{\tau}_1$ . The size of the

signal and, consequently, the estimated  $P_{\min}$  are practically independent of  $m_{\tilde{\chi}_1^0}$  (Fig. 2).

We have also noted that in spite of the combinatorial backgrounds, the invariant mass distribution of the above lepton-jet pair shows a peak at  $m_{\tilde{\tau}_1}$  (see Fig. 3). This peak, if discovered, will clearly establish the lepton number violating nature of the underlying interaction. Similarly the end point of the invariants mass distribution of the two lowest  $E_T$  jets (Fig. 4) which principally arise from LSP decays (Eq. (4)) may determine the LSP mass. Whether these salient features of the distributions will be obscured by the full SM background in the Tevatron data depends on the actual values of  $P$  and  $m_{\tilde{\tau}_1}$ .

This signal may turn out to be the main discovery channel even if the loop decay (Eq. (2)) of the  $\tilde{\tau}_1$ -NLSP (followed by the LSP decay) strongly dominates over its RPV decay (Eq. (1)). On the other hand if the RPV decay mode overwhelms the loop decay then the dilepton + dijet channel studied in [11–13] may provide a better signal. Finally if the data establish a competition between the two modes that would also be highly indicative of an underlying RPV model of neutrino mass. It may be recalled that in these models the neutrino oscillation data requires the  $\lambda'_{i33}$  couplings to be highly suppressed. As a result the two-body RPV decays have widths comparable to the competing RPC decays which occur in higher orders of perturbation theory if  $\tilde{\tau}_1$  is the NLSP.

The prospect of discovering the RPV model considered in this paper will be better if the RPV decays of  $\tilde{\tau}_1$  into final states with  $\tau + b$  can also be probed at the Tevatron. In fact scrutinizing these models in light of the oscillation data reveal that  $\tilde{\tau}_1 \rightarrow \tau^+ b$  is indeed the most dominant decay mode over a large region of the APS [17]. A model independent estimate of  $P_{\min}$  for this channel is, therefore, very important for a complete probe of this model.

Our computation of  $P$  in specific benchmark models [15,16] of neutrino oscillations establish that the APS filtered out by the oscillation data contain many points with  $P > P_{\min}$ . This happens both in the gauginolike (Fig. 5) and in the mixed model (Fig. 6). There are also regions in the APS where the dilepton + dijet signal proposed in [13] is unobservable but the signal proposed in this paper stands over the background. Thus the two signals are indeed complementary.

Since in the RPV MSSM leptons are baryons must be treated differently there is a basic incompatibility between this model and a typical GUT in which quarks and leptons are placed in the same multiplet. Thus RPV terms in the superpotential tend to violate both baryon and lepton number conservation and lead to catastrophic proton decays. Thus the task of a model builder is to remove such terms by introducing appropriate discrete symmetries [32]. Yet the RPV MSSM can be accommodated in the framework of a GUT. RPV interactions may, for example, be induced at the GUT scale by higher dimensional nonrenormalizable op-

erators which reduce to either baryon number or lepton number violating interactions when the GUT breaks down to the SM and certain heavy scalar fields develop vevs [33].

In GUT models neutrino masses can be generated at the weak scale in a variety of interesting ways. The set of input RPV parameters at  $M_G$  need not be identical to the set appearing in the neutrino mass matrix at the weak scale. In fact the former set may have a smaller number of parameters than the latter set. For example, one may start at  $M_G$  with three relatively large trilinear couplings different from the  $\lambda'_{i33}$ s required by the neutrino sector. Renormalization group evolution [34] and flavor violation inevitably present in any model due to the Cabibbo-Kobayashi-Maskawa (CKM) mixing would then induce the  $\lambda'_{i33}$  and the  $\mu_i$  parameters at the weak scale [35]. However, other RPV parameters may also be generated leading to a more complicated  $\nu$ -mass matrix. The relatively large input couplings may then lead to a rich low energy phenomenology [35] in addition to  $\tilde{t}_1$  and LSP decays. In this paper, however, we have not considered the origin of the weak

scale parameters and have restricted ourselves to the signatures of the  $\lambda'_{i33}$  couplings only.

The signal discussed in this paper and the one in Ref. [13] will certainly have much larger sizes at the LHC. But at higher energies many other sparticles may be produced as well. Thus one has to isolate the signal not only from the SM background but also from the SUSY background. On the other hand since the  $\tilde{t}_1$ -NLSP may very well be the only strongly interacting sparticle within the kinematic reach of the Tevatron. As a result these signals may be observed in a relatively clean environment.

## ACKNOWLEDGMENTS

S. P. thanks Dr. S. P. Das for computational help and Council of Scientific and Industrial Research (CSIR), India for support. A. D. acknowledges support from the Department of Science and Technology (DST), India under the Project No (SR/S2/HEP-18/2003).

- 
- [1] B. T. Cleveland *et al.*, *Astrophys. J.* **496**, 505 (1998); W. Hampel *et al.* (GALLEX Collaboration), *Phys. Lett. B* **447**, 127 (1999); M. Apollonio *et al.* (CHOOZ Collaboration), *Phys. Lett. B* **466**, 415 (1999); *Eur. Phys. J. C* **27**, 331 (2003); M. Altmann *et al.* (GNO Collaboration), *Phys. Lett. B* **490**, 16 (2000); Q. R. Ahmad *et al.* (SNO Collaboration), *Phys. Rev. Lett.* **87**, 071301 (2001); **89**, 011301 (2002); **89**, 011302 (2002); J. N. Abdurashitov *et al.* (SAGE Collaboration), *J. Exp. Theor. Phys.* **95**, 181 (2002); S. Fukuda *et al.* (Super-Kamiokande Collaboration), *Phys. Lett. B* **539**, 179 (2002); *Phys. Rev. Lett.* **89**, 011301 (2002); K. Eguchi *et al.* (KamLAND Collaboration), *Phys. Rev. Lett.* **90**, 021802 (2003); M. H. Ahn (K2K Collaboration) *Phys. Rev. Lett.* **90**, 041801 (2003).
- [2] For reviews on Supersymmetry, see, e.g., H. P. Nilles, *Phys. Rep.* **110**, 1 (1984); H. E. Haber and G. Kane, *Phys. Rep.* **117**, 75 (1985); J. Wess and J. Bagger, *Supersymmetry and Supergravity*, 2nd ed. (Princeton University, Princeton, NJ, 1991); M. Drees, P. Roy, and R. M. Godbole, *Theory and Phenomenology of Sparticles* (World Scientific, Singapore, 2005).
- [3] M. Gell-Mann, P. Ramond, and R. Slansky, in *Supergravity*, edited by D. Freedman and P. van Nieuwenhuizen (North-Holland, Amsterdam, 1979), p. 315; T. Yanagida, in *Proc. of the Workshop on Unified Theory and Baryon Number in the Universe*, edited by O. Sawada and A. Sugamoto (KEK, Japan, 1979); R. Mohapatra and G. Senjanovic, *Phys. Rev. Lett.* **44**, 912 (1980); *Phys. Rev. D* **23**, 165 (1981).
- [4] For a brief review see, e. g., S. Raby *Phys. Lett. B* **592**, 1 (2004), and references there in.
- [5] O. Gemonesi, *Int. J. Mod. Phys. A* **21**, 1887 (2006); K. Zuber, *J. Phys. G* **31**, S1471 (2005); S. M. Bilenky, *Phys. At. Nucl.* **69**, 2134 (2006); S. T. Petcov, *Phys. Scr.* **T121**, 94 (2005); M. Chemtob in [7]; Y. Uchida, *Phys. Lett. B* **537**, 256 (2002); M. Hirsch, H. V. Klapdor-Kleingrothaus, and S. G. Kovalenko, *Phys. Rev. D* **57**, 1947 (1998); *Phys. Rev. Lett.* **75**, 17 (1995).
- [6] For discussions on different models of  $\nu$ -mass see, e.g., Altarelli Ferruglio models of  $\nu$  mass G. Altarelli and F. Feruglio, *New J. Phys.* **6**, 106 (2004).
- [7] For reviews on RPV SUSY see, e. g., H. K. Dreiner, in *Perspectives on Supersymmetry*, edited by G. L. Kane (World Scientific, Singapore, to be published); A. Barbier *et al.*, *Phys. Rep.* **420**, 1 (2005); M. Chemtob, *Prog. Part. Nucl. Phys.* **54**, 71 (2005).
- [8] C. S. Aulakh and R. N. Mohapatra, *Phys. Lett. B* **119**, 136 (1982); L. Hall and M. Suzuki, *Nucl. Phys.* **B231**, 419 (1984); J. Ellis *et al.*, *Phys. Lett. B* **150**, 142 (1985); G. Ross and J. Valle, *Phys. Lett. B* **151**, 375 (1985); S. Dawson, *Nucl. Phys.* **B261**, 297 (1985); Y. Grossmann and H. E. Haber, *Phys. Rev. Lett.* **78**, 3438 (1997); *Phys. Rev. D* **59**, 093008 (1999).
- [9] For a recent review and further references see, e.g., S. Rakshit, *Mod. Phys. Lett. A* **19**, 2239 (2004).
- [10] Aseshkrishna Datta and B. Mukhopadhyaya, *Phys. Rev. Lett.* **85**, 248 (2000); D. Restrepo, W. Porod, and J. W. F. Valle, *Phys. Rev. D* **64**, 055011 (2001).
- [11] D. Acosta *et al.* (CDF collaboration), *Phys. Rev. Lett.* **92**, 051803 (2004).
- [12] S. Chakrabarti, M. Guchait, and N. K. Mondal, *Phys. Rev. D* **68**, 015005 (2003); *Phys. Lett. B* **600**, 231 (2004).
- [13] S. P. Das, Amitava Datta, and M. Guchait, *Phys. Rev. D* **70**, 015009 (2004).

- [14] V. Barger, G.F. Giudice, and T. Han, Phys. Rev. D **40**, 2987 (1989); G. Bhattacharyya, hep-ph/9709395; B.C. Allanach, A. Dedes, and H.K. Dreiner, Phys. Rev. D **60**, 075014 (1999).
- [15] A. Abada, M. Losada, Phys. Lett. B **492**, 310 (2000).
- [16] A. Abada, G. Bhattacharyya, and M. Losada, Phys. Rev. D **66**, 071701 (2002).
- [17] S.P. Das, Amitava Datta, and S. Poddar, Phys. Rev. D **73**, 075014 (2006).
- [18] K. Hikasa and M. Kobayashi, Phys. Rev. D **36**, 724 (1987).
- [19] C. Boehm, A. Djouadi, and Y. Mambrini, Phys. Rev. D **61**, 095006 (2000).
- [20] S.P. Das, A. Datta, and M. Guchait, Phys. Rev. D **65**, 095006 (2002).
- [21] S.P. Das, Phys. Rev. D **73**, 115004 (2006).
- [22] T. Sjostrand, P. Eden, C. Friberg, L. Lonnblad, G. Miu, S. Mrenna, and E. Norrbin, Comput. Phys. Commun. **135**, 238 (2001); For a more recent version, see J. High Energy Phys. 05 (2006) 026.
- [23] See, e.g., A. Pukhov, hep-ph/9908288; For the more recent versions see: <http://www.ifh.de/pukhov/calchep.html>.
- [24] G. Kane and J.P. Leveille, Phys. Lett. B **112**, 227 (1982); P.R. Harrison and C.H. Llewellyn-Smith, Nucl. Phys. **B213**, 223 (1983); S. Dawson, E. Eichten, and C. Quigg, Phys. Rev. D **31**, 1581 (1985); E. Reya and D.P. Roy, Phys. Rev. D **32**, 645 (1985); H. Baer and X. Tata, Phys. Lett. B **160**, 159 (1985).
- [25] H.L. Lai *et al.* (CTEQ Collaboration), J. High Energy Phys. 07 (2002) 012.
- [26] M. Cacciari *et al.*, J. High Energy Phys. 04 (2004) 68; N. Kidonakis and R. Vogt, Phys. Rev. D **68**, 114014 (2003).
- [27] W. Beenakker, M. Kramer, T. Plehn, M. Spira, and P.M. Zerwas, Nucl. Phys. **B515**, 3 (1998).
- [28] For neutrino oscillation data, see, e.g., M. Maltoni *et al.*, New J. Phys. **6**, 122 (2004).
- [29] S. Davidson and M. Losada, J. High Energy Phys. 05 (2000) 021; Phys. Rev. D **65**, 075025 (2002).
- [30] See e.g., J.M. Frere, D.R.T. Jones, and S. Raby, Nucl. Phys. **B222**, 11 (1983); M. Claudson, L.J. Hall, and I. Hinchliffe, Nucl. Phys. **B228**, 501 (1983); J.A. Casas, A. Lleyda, and C. Munoz, Nucl. Phys. **B471**, 3 (1996).
- [31] J.F. Gunion and H.E. Haber, Phys. Rev. D **37**, 2515 (1988).
- [32] L.J. Hall and M. Suzuki, in [8].
- [33] D.E. Brahm and L.J. Hall, Phys. Rev. D **40**, 2449 (1989); K. Tamvakis, Phys. Lett. B **382**, 251 (1996); C.S. Aulakh *et al.* Nucl. Phys. **B597**, 89 (2001); D.G. Lee and R.N. Mohapatra, Phys. Rev. D **51**, 1353 (1995); G.F. Giudice and R. Rattazzi, Phys. Lett. B **406**, 321 (1997).
- [34] R. Hempfling, Nucl. Phys. **B478**, 3 (1996); M. Hirsch *et al.*, Phys. Rev. D **62**, 113008 (2000); **65**, 119901(E) (2002); B. de Carlos and P.L. White, Phys. Rev. D **54**, 3427 (1996); **55**, 4222 (1997); H.K. Dreiner *et al.*, Phys. Rev. D **69**, 053002 (2004).
- [35] A. Datta, J.P. Saha, A. Kundu, and A. Samanta, Phys. Rev. D **72**, 055007 (2005).